J|A|C|S
ARTICLES

Published on Web 12/08/2008

The Second Step of the Nitric Oxide Synthase Reaction: Evidence for Ferric-Peroxo as the Active Oxidant

Joshua J. Woodward, Michelle M. Chang, Nathaniel I. Martin,† and Michael A. Marletta*

Departments of Chemistry, Molecular and Cellular Biology, QB3 Institute, and Division of Physical Biosciences, Lawrence Berkeley National Laboratory, University of California, Berkeley, California 94720-3220

Received September 15, 2008; E-mail: marletta@berkeley.edu

Abstract: Nitric oxide synthase (NOS) is a P450 mono-oxygenase that catalyzes the oxidation of L-arginine to citrulline and NO through the stable intermediate N^G-hydroxy-L-arginine (NHA). The oxidation of NHA by NOS is unique. There is little direct evidence in support of the nature of the heme bound oxidant [i.e., ferric-peroxo vs Fe^{IV}=O(por$^{\bullet+}$)] responsible for this transformation. Previous work characterizing the H_2O_2-driven oxidation of NHA by NOS showed the formation of citrulline and the side product N^δ-cyanoornithine (CN-orn). This led to the proposed involvement of a ferric-peroxo intermediate in the oxidation of NHA to citrulline. To test this hypothesis we used this model reaction to study the effects of pH, heme substitution, active site mutagenesis, and a fluorinated substrate analogue on the product distribution. Further, the oxidation of 2,2′-azino-bis(3-ethylbenzthiazoline-6-sulfonic acid) (ABTS) by H_2O_2 and $iNOS_{heme}$ was used to probe the protein-catalyzed breakdown of peroxide to the Fe^{IV}=O(por$^{\bullet+}$) intermediate. At pH 6.5, 7.5, and 8.5 the peroxide shunt reaction forms 26 ± 2, 36 ± 1, and 51 ± 1% citrulline, respectively. The rate of peroxidase activity, however, was negatively correlated to pH, with a peroxide breakdown rate of 13.1 ± 0.3, 8.3 ± 0.2, and 4.2 ± 0.1 M^{-1} s^{-1} at pH 6.5, 7.5, and 8.5, respectively. Mutation of active site valine 346 to an alanine shifted the product distribution to 5.2 ± 0.5% citrulline while enhancing the peroxide cleavage rate to 14.3 ± 0.7 M^{-1} s^{-1}. Substitution of the heme cofactor with iron mesoporphyrin IX (Fe-MPIX) alters the product distribution from 36 ± 1% citrulline to 22 ± 3% citrulline. Metal substitution with Mn results in the formation of 64.7 ± 0.8% citrulline. Conversely, the electrophilic 4,4-difluoro-N^G-hydroxy-L-arginine substrate analogue shifted the product distribution to 68.6 ± 0.6% 4,4-difluorocitrulline. The peroxidase data provide insight into the chemical features of NOS that control the processing of the ferric-peroxo species to the Fe^{IV}=O(por$^{\bullet+}$) intermediate and help interpret the product distributions observed for the peroxide shunt under various conditions. In all cases, the ability of the protein to break down peroxide is negatively correlated with the formation of citrulline by the peroxide shunt. These results support the high valent Fe^{IV}=O(por$^{\bullet+}$) intermediate as the species responsible for CN-orn formation and are consistent with the involvement of the ferric-peroxo intermediate in the oxidation of NHA to citrulline.

Nitric oxide (NO) is an important biological molecule with central roles in processes as diverse as cellular signaling and in the host innate immune response to infection. Because of this widespread biological activity, nitric oxide synthase (NOS), the enzyme responsible for NO biosynthesis, has been the focus of many investigations. Specifically, a detailed understanding of the mechanism by which NOS catalyzes the formation of NO has been a central focus because of the potential therapeutic utility.

NOS is a multicofactor, multidomain protein that oxidizes substrate arginine to the products citrulline and NO. This transformation proceeds through two successive oxidative steps carried out by a P450 type heme using O_2 and nicotinamide adenine dinucleotide phosphate (NADPH) as cosubstrates and with N^G-hydroxy-L-arginine (NHA) as a stable intermediate (Scheme 1).[1]

Scheme 1. NOS Reaction

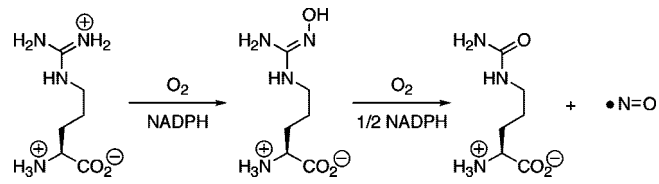

The reductase domain utilizes two flavin cofactors to transfer electrons from NADPH to the heme domain. As is characteristic of P450s, oxygen is activated through a two-electron reduction at the heme cofactor of NOS, yielding a ferric-peroxo intermediate (Scheme 2, steps a−d, see ref 2 for review of P450 chemistry). Unique to NOS, however, a pterin cofactor acts as the donor for the second electron during oxygen activation (Scheme 2, step d). The resulting ferric-peroxo species can undergo successive protonation events on the distal oxygen, followed by heterolytic bond cleavage to form a high valent

† Present address: Department of Chemistry, University of Utrecht, The Netherlands.

10.1021/ja807299t CCC: $40.75

Scheme 2. P450 Reaction Cycle[a]

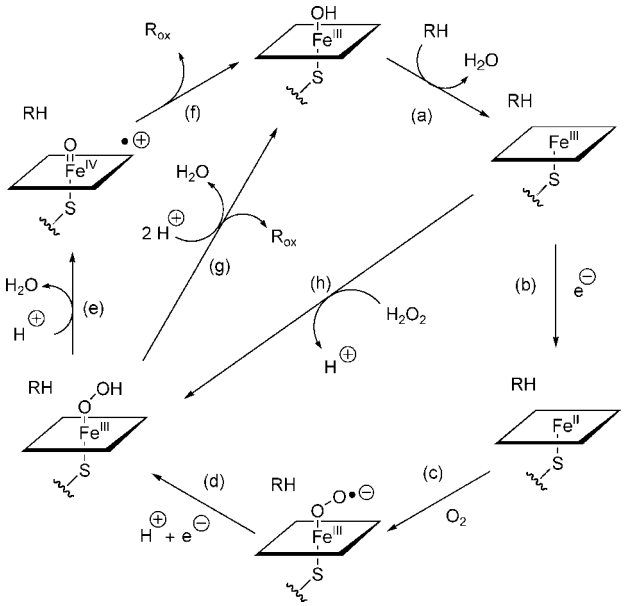

[a] The proposed reaction cycle of P450s including NOS is presented. Oxygen is activated to a ferric-peroxo intermediate using two electrons (steps a−d). This intermediate can undergo heterolytic oxygen−oxygen bond cleavage to yield a high valent Fe^{IV}═O(por$^{\bullet+}$), which can act as the active oxidant in substrate oxidation (steps e and f). Conversely, the ferric-peroxo intermediate may act as a nucleophilic oxidant, directly oxidizing the substrate (step g). The use of H_2O_2 in place of molecular oxygen and electrons allows for the direct formation of the ferric-peroxo intermediate from the ferric resting state of the protein (step h). RH, substrate. R_{ox}, oxidized substrate.

Fe^{IV}═O(por$^{\bullet+}$) species as the substrate oxidant (Scheme 2, steps e−f) or it can act as a nucleophilic oxidant directly (Scheme 2, step g).[3]

Currently, there is limited evidence implicating either a ferric-peroxo or a high valent Fe^{IV}═O(por$^{\bullet+}$) intermediate as the active oxidant in the transformation of NHA to citrulline (Scheme 3). The delivery of the second electron to the ferric superoxo species is rate limiting and kinetically masks the observation of subsequent intermediates. Thermal annealing EPR and ENDOR spectroscopy have led to the direct observation of a ferric-peroxo species; however, no Fe^{IV}═O(por$^{\bullet+}$) intermediate was detected.[4] This result, however, does not exclude the involvement of an Fe^{IV}═O(por$^{\bullet+}$) intermediate because the ferric-peroxo species is a precursor, and accumulation of the high valent species may not be resolved by thermal annealing.

Continuous-flow resonance Raman spectroscopy was used to report the hydrogen bonding pattern to the oxygen bound heme.[5] Contrary to reactions with arginine, no hydrogen bonding to the distal oxygen was observed with NHA. These results suggest that following electron transfer to the ferric-superoxo intermediate (Scheme 2, step d) the resulting ferric-peroxo species will not be set up to undergo further processing to a high valent Fe^{IV}═O(por$^{\bullet+}$) intermediate, suggesting that a ferric-peroxo is the oxidant in the second step.

Because the slow rate of superoxide reduction prevents the direct observation of the involved intermediates, we have chosen to use chemical techniques to probe the nature of the active oxidant in the transformation of NHA to citrulline. The chemical similarity of two-electron reduced molecular oxygen and hydrogen peroxide allows for shunting of P450s (Scheme 2, step h). This process has been described for a number of P450 reactions, including the oxidation of NHA by NOS.[6,7] In the latter case, however, the reaction does not result in the typical products observed when O_2 and NADPH are used. Instead, the reaction products contain nitroxyl and other inorganic nitrogen oxides (NO_2^-/NO_3^-), as well as a distribution of cyano-ornithine (CN-orn) and citrulline.

The appearance of a new amino acid product in the peroxide shunt reaction is indicative of flux through a "non-natural" oxidative reaction pathway. The increase in acidity of the active site from the use of hydrogen peroxide as opposed to two-electron reduced molecular oxygen may facilitate the breakdown of the ferric-peroxo intermediate to the Fe^{IV}═O(por$^{\bullet+}$), resulting in the formation of CN-orn. If true, this suggests the involvement of a ferric-peroxo species in the formation of citrulline (Scheme 4).[7]

Here the peroxide shunt product distribution is measured under a range of conditions to better understand the conditions that favor citrulline formation. In parallel, we characterize the peroxidase activity of NOS to monitor the ability of the protein to break down peroxide to the high valent Fe^{IV}═O(por$^{\bullet+}$) intermediate. Together, these results advance our understanding of the NOS activation of the peroxide O—O bond and provide strong evidence in support of a ferric-peroxo intermediate as the active oxidant for citrulline formation.

Materials and Methods

Materials and General Methods. Iron mesoporphyrin IX (Fe-MPIX) was purchased from Frontier Scientific. Terrific Broth culture media and isopropyl-β-D-thiogalactoside (IPTG) were from Research Products International. Carbenicillin was from MP Biomedicals. Centrifugal concentrators were obtained from Millipore. Ni-NTA Superflow resin and Spin Miniprep Kits were obtained from Qiagen. All water used was 18 mΩ from a Milli-Q Ultrapure Water Purification System (Millipore). HPLC solvents were from Fisher Scientific. (6*R*)-5,6,7,8-Tetrahydro-L-biopterin (H_4B) was purchased from Schirck's Laboratory. 4,4-Difluoro-N^G-hydroxy-L-arginine (DF-NHA) was synthesized as described previously.[8] All other chemicals and reagents were purchased from Sigma-Aldrich.

Protein samples were reconstituted with H_4B by incubating with H_4B (500 μM) and DTT (dithiothreitol, 5 mM) for 1 h on ice as described previously.[9] Samples were subsequently desalted and concentrated to >100 μM, as determined by UV−visible absorption spectroscopy. Hydrogen peroxide solutions were made fresh each day from a concentrated stock (30%). H_2O_2 concentrations were determined by monitoring the absorbance at 240 nm (ϵ = 39.4 M^{-1} cm^{-1}).[10]

(1) White, K. A.; Marletta, M. A. *Biochemistry* **1992**, *31*, 6627–6631.
(2) Sono, M.; Roach, M. P.; Coulter, E. D.; Dawson, J. H. *Chem. Rev.* **1996**, *96*, 2841–2888.
(3) Vaz, A. D.; Pernecky, S. J.; Raner, G. M.; Coon, M. J. *Proc. Natl. Acad. Sci. U.S.A.* **1996**, *93*, 4644–4648.
(4) Davydov, R.; Ledbetter-Rogers, A.; Martasek, P.; Larukhin, M.; Sono, M.; Dawson, J. H.; Masters, B. S.; Hoffman, B. M. *Biochemistry* **2002**, *41*, 10375–10381.
(5) Li, D.; Kabir, M.; Stuehr, D. J.; Rousseau, D. L.; Yeh, S. R. *J. Am. Chem. Soc.* **2007**, *129*, 6943–6951.
(6) Pufahl, R. A.; Wishnok, J. S.; Marletta, M. A. *Biochemistry* **1995**, *34*, 1930–1941.
(7) Clague, M. J.; Wishnok, J. S.; Marletta, M. A. *Biochemistry* **1997**, *36*, 14465–14473.
(8) Martin, N. I.; Woodward, J. J.; Marletta, M. A. *Org. Lett.* **2006**, *8*, 4035–4038.
(9) Hurshman, A. R.; Krebs, C.; Edmondson, D. E.; Huynh, B. H.; Marletta, M. A. *Biochemistry* **1999**, *38*, 15689–15696.
(10) Nelson, D. P.; Kiesow, L. A. *Anal. Biochem.* **1972**, *49*, 474–478.

Scheme 3. Proposed Mechanisms of NHA Oxidation by NOS[a]

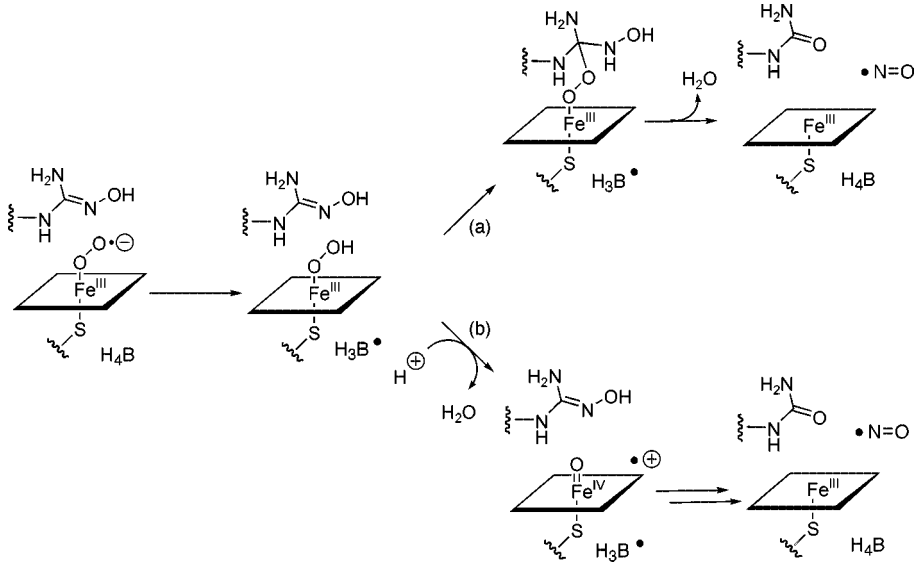

[a] Two possible heme bound oxidants may be responsible for catalyzing the transformation of NHA to citrulline and NO. (a) A ferric-peroxo species may act as a nucleophilic oxidant directly attacking substrate NHA, or (b) the ferric-peroxo intermediate can undergo further processing to a high valent Fe^{IV}=O($por^{\bullet+}$) intermediate which may oxidize NHA.

Scheme 4. Proposed Mechanism of NOS Peroxide Shunt[a]

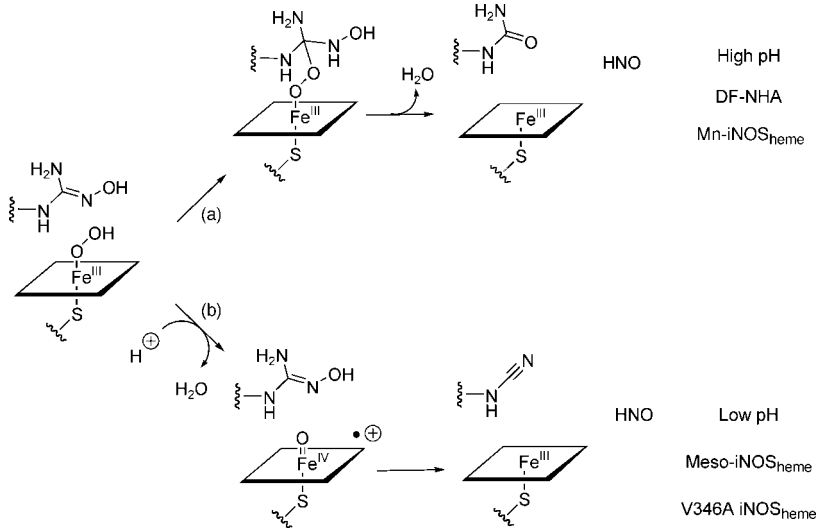

[a] Two competing reactions are proposed for the NOS peroxide shunt oxidation of NHA. Direct nucleophilic attack of the ferric-peroxo species on the substrate leads to the formation of citrulline (path a). H_2O_2 oxygen−oxygen bond cleavage to form the high valent Fe^{IV}=O($por^{\bullet+}$) intermediate leads to the formation of CN-orn (path b). Elevated pH, the use of Mn substituted iNOS$_{heme}$, and the use of an electrophilic substrate analogue (DF-NHA) enhance nucleophilic attack of the substrate by a ferric-peroxo intermediate to give more citrulline product. Pterin-free protein in low pH buffer or that contains an active site mutation (V346A iNOS$_{heme}$) enhances peroxide breakdown to the high valent Fe^{IV}=O($por^{\bullet+}$) species as monitored by ABTS oxidation. Together with the use of heme-substituted protein (Meso-iNOS$_{heme}$), these active site changes also exhibit enhanced formation of CN-orn during the peroxide shunt.

Protein Expression and Purification. Heme substituted iNOS$_{heme}$ was generated using the method developed in our laboratory for incorporation of non-natural porphyrins into proteins during their expression.[11] The V346A iNOS$_{heme}$ DNA construct was made using the QuikChange method of mutagenesis with the following primers: 5′ - GTG GTA TGC ACT GCC TGC CGC AGC CAA CAT GCT ACT GGA G - 3′ and 5′ - CTC CAG TAG CAT GTT GGC TGC GGC AGG CAG TGC ATA CCA C - 3′ with pCW iNOS$_{heme}$ as the template DNA. DNA sequencing was performed by the UC Berkeley DNA sequencing facility. The plasmid variant was used to transform chemically competent JM109 cells, and protein expression was performed as reported previously.[9] Purification of wild-type, heme-substituted, and variant iNOS$_{heme}$ was accomplished using Ni-NTA and anion exchange chromatography as previously described.[11]

Peroxidase Activity Assays. The peroxidase activity of WT and heme substituted iNOS$_{heme}$ was measured using the common peroxidase reporter substrate ABTS (2,2′-azino-bis(3-ethylbenzthiazoline-6-sulfonic acid)). Formation of the oxidation product, $ABTS^{\bullet+}$, was monitored at the λ_{max} of 414 nm (ϵ = 36 mM^{-1} cm^{-1}).[12] Protein stocks were thawed and desalted using a PD10 column (GE Healthcare) to exchange into HEPES (4-(2-hydroxyethyl)-1-piperazineethanesulfonic acid) reaction buffer. Reaction pH

(11) Woodward, J. J.; Martin, N. I.; Marletta, M. A. *Nat. Methods* **2007**, *4*, 43–45.

(12) Childs, R. E.; Bardsley, W. G. *Biochem. J.* **1975**, *145*, 93–103.

was maintained using the appropriate buffer (100 mM HEPES pH 6.5, 7.5, and 8.5). All reactions were initiated by the addition of H_2O_2. First-order dependence with respect to enzyme was confirmed by showing a linear increase in rate with respect to enzyme concentration (Supporting Information). Reactions were performed with varying ABTS or H_2O_2. For experiments with varied H_2O_2, NOS (0.5−2 μM) and ABTS (1 mM) in HEPES buffer were mixed with an equal volume of hydrogen peroxide (0−200 mM) in HEPES buffer. Spectral transitions were monitored on a Hi-Tech SF-61 Stopped Flow Spectrophotometer equipped with a diode array absorbance detector and a temperature controlled water bath set to 10 °C. Conversely, reactions with varied ABTS concentration (0−4 mM) contained constant 50 mM peroxide and were monitored as described above.

Peroxide Shunt Amino Acid Product Analysis. Peroxide shunt reactions were performed as described previously.[7] Pterin-reconstituted protein samples (wild type, V346A, and Fe-MPIX substituted $iNOS_{heme}$, 1−3 μM) were mixed with H_4B ((6*R*)-5,6,7,8-tetrahydro-L-biopterin, 50 μM), NHA (N^G-hydroxy-L-arginine) or DF-NHA (1 mM), and HEPES (100 mM, pH 7.5) ($iNOS_{heme}$, heme oxygenase domain of murine inducible nitric oxide synthase (amino acids 1−490)). Reactions were initiated with the addition of H_2O_2 to a final concentration of 100 mM at room temperature. At various time points (0−1.5 min) reactions were quenched by the addition of catalase (2.5 mg/mL final concentration). Amino acids in the reaction mixture were derivatized by naphthalene-2,3-dicarboxaldehyde (NDA) and quantified by reversed phase HPLC. Samples containing NHA were eluted as described previously.[13] Samples containing the substrate analogue 4,4-difluoro-N^G-hydroxy-L-arginine (DF-NHA) were analyzed using an Agilent 1100 series liquid chromatography/mass selective detector (LC/MSD). Solvent A was ammonium acetate (5 mM, pH 6.0) with 20% MeOH. Solvent B was MeOH. The column was developed with a gradient from 10−50% Solvent B over 9 min, 50−100% B over 2 min, 100% B for 3 min, to finally a return to 10% B over 0.5 min. The column was washed for 5 min at 10% B between each run. Under these conditions retention times are as follows: 4,4-difluoro-citrulline (DF-citrulline), 9.7 min; 4,4-difluoro-N^δ-cyanoornithine (DF-CN-orn), 10.6 min; DF-NHA, 11.9 min; phenylalanine, 13.7 min. Electrospray mass spectra (m/z = 100−1000) were collected for each peak to ensure proper identification of the eluting species.

Results and Discussion

Initial Characterization of $iNOS_{heme}$ Peroxidase Activity. Hydrogen peroxide provides access to both of the proposed active oxidants of the P450 reaction cycle, specifically the ferric-peroxo and the Fe^{IV}=O(por$^{\bullet+}$)/Compound I (Cpd I) intermediates. No significant buildup of these intermediates is observed during O_2/NADPH (NADPH, nicotinamide adenine dinucleotide phosphate) or H_2O_2 driven oxidation of NHA. Without the use of spectroscopic techniques, discriminating between these two species is difficult due to their high reactivity. As a result, assigning the involvement of each intermediate in various chemical transformations has not been possible.

Peroxidases catalyze the breakdown of H_2O_2 to a Cpd I intermediate and then catalyze the sequential single electron oxidation of two substrate molecules (Scheme 5). A number of colorimetric reporter substrates have been developed for the kinetic study of these reactions, with ABTS perhaps being the most common. Because ABTS has significant reactivity with Cpds I and II (the product of the first reduction of Cpd I by ABTS; refer to Scheme 5) and not with peroxide in solution, we hypothesized that if NOS and H_2O_2 could drive the oxidation of ABTS, we could use this reporter substrate to quantify the rate of formation of Cpd I by NOS.

Scheme 5. General Mechanism for a Peroxidase-Catalyzed Reaction[a]

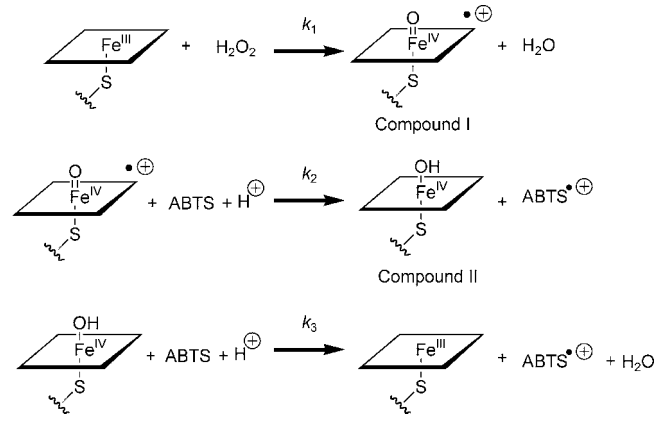

[a] In the accepted peroxidase mechanism, H_2O_2 undergoes oxygen−oxygen bond heterolysis at the heme center to form the compound I intermediate and water. The compound I species then performs a single electron oxidation on one substrate molecule to yield a substrate radical cation and compound II. After another single electron oxidation of a second substrate molecule, the protein returns to the resting ferric state.

In the presence of H_2O_2, NOS catalyzes the oxidation of ABTS to a radical cation. As monitored by UV−visible absorption spectroscopy, this reaction was linear for a short time (~2 s) followed by an exponential decrease in activity over the time course examined (Figure 1a). Addition of fresh enzyme to reactions no longer exhibiting a change in absorbance restores activity, indicative of time dependent irreversible enzyme deactivation (Supporting Information). The rate of this deactivation is proportional to the concentration of H_2O_2. Therefore, stopped-flow spectroscopy was required to obtain accurate initial rates for H_2O_2 concentrations above 5 mM.

Due to the constant rate of enzyme deactivation, progress curves were fit to eq 1 (see Supporting Information for derivation), where P is the product as a function of time, A is the final concentration of product produced at infinite time, k_{obs} is the observed rate constant for deactivation, and C is the t = 0 correction for background ABTS absorbance. As purchased, ABTS contains a small portion of ABTS$^{\bullet+}$, and increasing concentrations in each reaction lead to a proportional increase in background absorbance at t = 0, necessitating the use of the absorbance correction C.

$$P(t) = A(1 - e^{-k_{obs}t}) + C \quad (1)$$

$$v_i = \frac{d[P]}{dt}(0) = Ak_{obs} \quad (2)$$

In this reaction, H_2O_2 acts as both a substrate and an irreversible inhibitor of NOS. Equation 1 accounts for the exponential decay of catalytically active enzyme at constant [H_2O_2]. At time zero, the derivative of eq 2 is equal to the product of the two constants, A and k_{obs}, determined from fitting primary data to eq 1. Initial rates (v_i) were calculated in this manner.

Scheme 5 depicts the accepted reaction mechanism of peroxidases, where enzyme reacts with H_2O_2 to form a compound I intermediate that carries out two successive oxidations on separate substrate molecules.[14] Under steady state conditions, the activity is described by the generally accepted equation of Dunford et al. (eqs 3 and 4; see Supporting

(13) Hurshman, A. R.; Marletta, M. A. *Biochemistry* **2002**, *41*, 3439–3456.

(14) Dunford, H. B. *Xenobiotica* **1995**, *25*, 725–733.

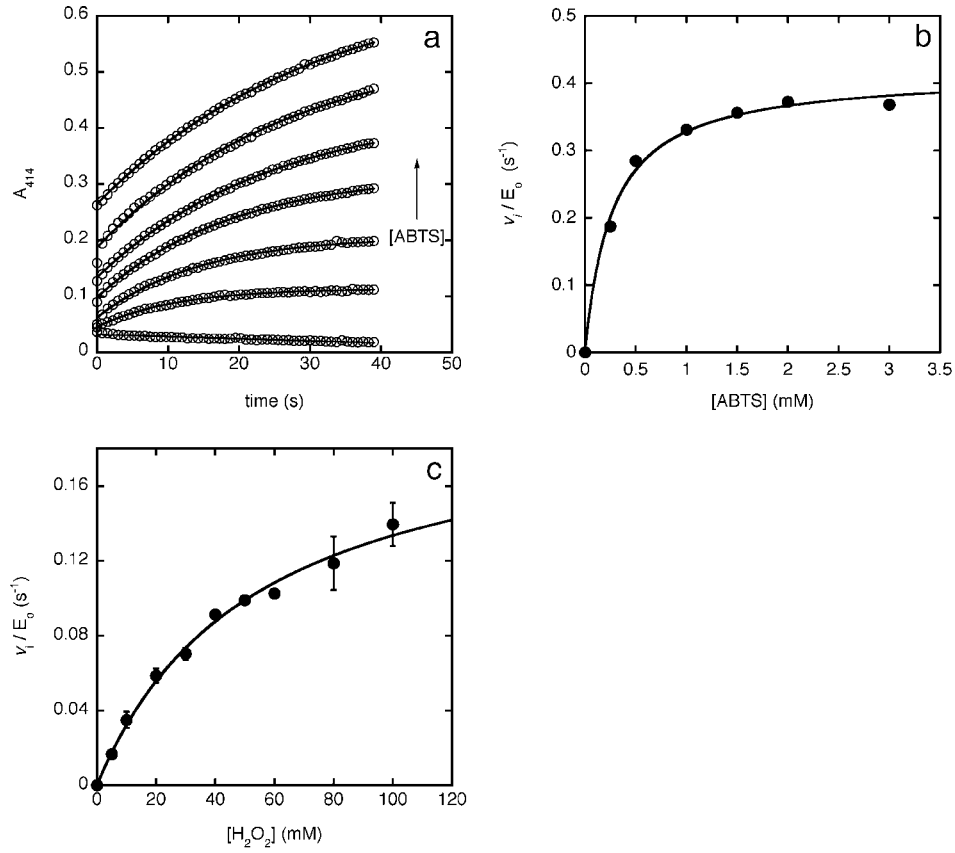

Figure 1. ABTS peroxidase activity of $iNOS_{heme}$. Characterization of the peroxidase reaction catalyzed by nitric oxide synthase with ABTS. (a) Representative fit of progress curves to eq 1. Reactions contain $iNOS_{heme}$ (0.5 μM), HEPES (pH 7.5, 100 mM), H_2O_2 (50 mM), and ABTS (0, 0.25, 0.5, 1, 1.5, 2, and 3 mM) at 10 °C. (b) Rate of ABTS oxidation versus ABTS concentration. Reactions contain 0.5 μM $iNOS_{heme}$, 0 − 3 mM ABTS, and 50 mM H_2O_2 at 10 °C. (c) Rate of ABTS oxidation versus peroxide concentration. Reactions consist of 0.7 μM $iNOS_{heme}$, 0−100 mM H_2O_2, 0.25 mM ABTS, and 100 mM HEPES (pH 7.5) at 10 °C.

Information for derivation), where v_i is the initial rate of the reaction, k_1 and k_3 are the rates as described in Scheme 5, and E_o is the initial enzyme concentration.[15] Equations 3 and 4 predict saturation behavior for both ABTS and H_2O_2 as each substrate is varied. When ABTS was varied and H_2O_2 was held constant, the reaction showed saturation type kinetics (Figure 1b), as predicted. When H_2O_2 was varied and ABTS was held constant, saturation behavior was also observed. However, only partial saturation was attained even at 100 mM H_2O_2 (Figure 1c).

$$v_i = \frac{2E_o k_3[H_2O_2][ABTS]}{[H_2O_2] + (k_3/k_1)[ABTS]} \quad (3)$$

$$v = \frac{2E_o k_1[H_2O_2][ABTS]}{(k_1/k_3)[H_2O_2] + [ABTS]} \quad (4)$$

When H_2O_2 is held constant and ABTS is varied (eq 4), initial rates saturate at k_1, providing a quantifiable measure of the rate of H_2O_2 breakdown catalyzed by NOS. It is important to note that the rate obtained contains both the equilibrium constant for peroxide binding and the unimolecular rate constant for the rate-limiting step of O−O bond scission. To compare the peroxidase activity under various conditions, H_2O_2 concentrations were held constant at 50 mM while ABTS was varied. Bimolecular rate constants describing the rate of H_2O_2 breakdown (k_1) were determined by fitting normalized initial rates (v_i/E_o) as a function of ABTS concentration to eq 4. The half-saturation concentration is proportional to the ratio of k_1 to k_3. Under all conditions measured $k_3 > 150\ k_1$, indicating that the observed saturation rate is primarily dictated by k_1 under steady state conditions (Table 1).

Table 1. Peroxidase Rates and Citrulline Product Formation

reaction contents	peroxidase rate k_1 (M^{-1} s^{-1})	$(k_3/k_1)^b$	% citrulline
WT $iNOS_{heme}$			
pH 6.5	13.1 ± 0.3	190 ± 20	26 ± 2
pH 7.5	8.3 ± 0.2	240 ± 30	36 ± 1
pH 8.5	4.2 ± 0.1	190 ± 20	51 ± 1
DF-NHA[a]	NA[c]	NA[c]	68.6 ± 0.6
Meso-$iNOS_{heme}$[a]	NM[c]	NM[c]	22 ± 3
Mn-$iNOS_{heme}$	ND[c]	NM[c]	64.7 ± 0.8
V346A $iNOS_{heme}$[a]	14.3 ± 0.7	230 ± 50	5.2 ± 0.5

[a] DF-NHA, Meso-$iNOS_{heme}$, and V346A $iNOS_{heme}$ were examined at pH 7.5. [b] Ratio of measured rate constants reported as the value ± the fit error obtained from fitting initial rate data to Equation 4. [c] NA, not applicable; NM, not measurable; ND, none detected.

Peroxide Shunt Reactions. Peroxide shunt reactions were performed as reported for the full-length NOS.[7] Pterin free enzyme produces multiple reaction products, including CN-orn, citrulline, and an unidentified amino acid product similar to that observed during dithionite driven turnover of NHA by pterin-

(15) Rasmussen, C. B.; Dunford, H. B.; Welinder, K. G. *Biochemistry* **1995**, *34*, 4022–4029.

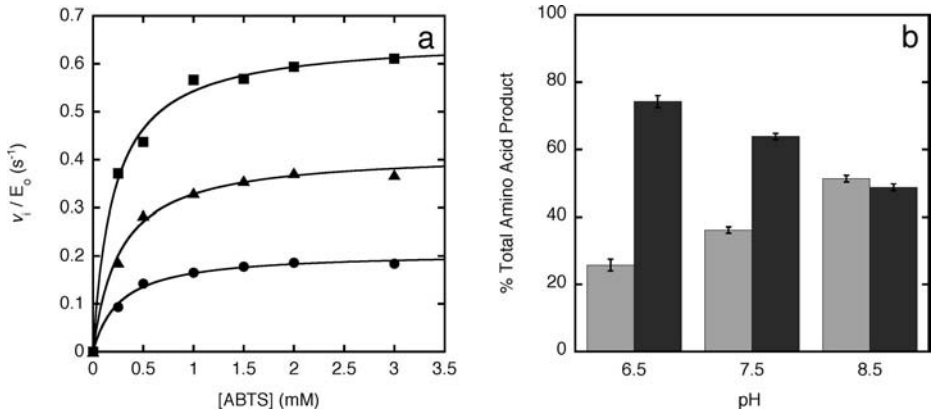

Figure 2. Effect of pH on peroxidase activity and peroxide shunt product distribution. (a) pH dependence of steady state peroxidase activity. Reactions contain $iNOS_{heme}$ (0.5 μM), H_2O_2 (50 mM), pH 6.5 (-■-), pH 7.5 (-▲-), or pH 8.5 (-●-) HEPES (100 mM), and ABTS (0−3 mM) at 10 °C. Initial rates (v_i) as determined by steady state analysis are normalized to enzyme concentration (E_o) and plotted as a function of ABTS substrate concentration. (b) pH dependence of the formation of citrulline (light gray) and CN-ornithine (dark gray). Reactions contain $iNOS_{heme}$ (2 μM), NHA (1 mM), H_2O_2 (100 mM), and HEPES (100 mM, pH 6.5, 7.5, or 8.5). Amino acid products are the average of three measures and reported as the percent of the total amino acid formed as determined by NDA derivatization and HPLC quantification.

free $iNOS_{heme}$ (Supporting Information).[16] Following H_4B reconstitution, desalting, and treatment with H_2O_2 a small amount of the unidentified amino acid product was observed. However, upon addition of excess pterin, only CN-orn and citrulline were observed as products, suggestive of full binding of pterin to the protein. Likely, a portion of pterin is lost from the protein during the desalting step and the addition of a small excess of H_4B results in full reconstitution.

The activation of the O−O bond of H_2O_2 at ferric heme can proceed without the input of additional electrons. Without the need to provide electrons to activate oxygen,[16,17] pterin radical formation is not predicted. The inorganic reaction products of the peroxide shunt contain nitroxyl and other inorganic nitrogen oxides. The overall input of two electrons from H_2O_2, rather than the one as occurs during normal turnover, changes the electron stoichiometry and is consistent with the formation of HNO rather than NO. Other nitrogen oxides, mainly nitrite and nitrate, are also observed and have been postulated to occur as a result of oxidation of nitroxyl from peroxide or oxygen.[6] As a result, the role of the pterin in the peroxide-NHA reaction is likely only structural, not catalytic.

pH Effects on H_2O_2 Reactions. The use of H_2O_2 in place of O_2 and NADPH should increase the acidity of the active site. More acidic conditions are likely to favor the heterolysis of the peroxide bound heme to form Cpd I (Scheme 4, path b). Therefore, the rate of peroxide cleavage (k_1, Scheme 5) catalyzed by $iNOS_{heme}$ was measured as a function of pH to determine the role of protons in NOS catalyzed H_2O_2 decomposition.

A clear dependence of k_1 on pH is observed, with greater rates of catalysis at lower pH (Figure 2a and Table 1). This is consistent with the proposal that that H_2O_2 breakdown is a proton-driven process. Proton delivery to the distal oxygen is required to induce heterolytic oxygen cleavage. In natural peroxidases, an active site catalytic residue often acts to mediate proton transfer from the proximal to the distal oxygen, facilitating O−O bond heterolysis. However, the NOS active site does not contain any obvious candidates that could serve as a general acid. It then stands to reason that ferric-bound peroxide breakdown is dependent on a solvent-derived proton and that this pathway is directly dependent on solvent pH.

The observed effect of pH on the peroxidase activity of NOS suggests that at low pH there is an enhancement in the peroxide O−O bond heterolysis, facilitating the formation of the Cpd I intermediate. If the proposed mechanism outlined in Scheme 4 is correct, then more acidic conditions are expected to increase CN-orn formation. Similar to the peroxidase activity, a marked trend in the product distribution was observed (Figure 2b, Table 1). The relative amount of citrulline increased with pH at the expense of CN-orn. Coupling the peroxide cleavage data with the product distribution reveals that faster peroxide decomposition correlates to increased formation of CN-orn. These data are consistent with the mechanistic hypothesis that peroxide breakdown results in the formation of an Fe^{IV}═O($por^{\bullet+}$) intermediate, which then oxidizes NHA to CN-orn. Proton access to the ferric-bound peroxide appears to be a determining factor in committing the protein down separate reaction pathways that ultimately result in the formation of citrulline or CN-orn.

Active Site Mutagenesis. Recent crystallographic studies suggest that an ordered active site water may act as a proton donor or may facilitate proton delivery from solvent.[18−20] In light of this, we reasoned that the observed pH dependence of the peroxidase activity rests on the ability of solvent water to access the active site.

Val 346 is a conserved residue that is positioned at the entrance of the active site of the eukaryotic NOSs (Figure 3a). Previous work has shown that this amino acid plays an important role in regulating movement into and out of the heme pocket.[21,22] Here, we characterize peroxidase reactions of V346A $iNOS_{heme}$, a mutant designed to provide increased solvent access to the active site (Figure 3a and b). Consistent with solvent involve-

(16) Hurshman, A. R.; Krebs, C.; Edmondson, D. E.; Marletta, M. A. *Biochemistry* **2003**, *42*, 13287–13303.
(17) Wei, C. C.; Wang, Z. Q.; Hemann, C.; Hille, R.; Stuehr, D. J. *J. Biol. Chem.* **2003**, *278*, 46668–46673.
(18) Fedorov, R.; Ghosh, D. K.; Schlichting, I. *Arch. Biochem. Biophys.* **2003**, *409*, 25–31.
(19) Li, H.; Igarashi, J.; Jamal, J.; Yang, W.; Poulos, T. L. *J. Biol. Inorg. Chem.* **2006**, *11*, 753–768.
(20) Martin, N. I.; Woodward, J. J.; Winter, M. B.; Beeson, W. T.; Marletta, M. A. *J. Am. Chem. Soc.* **2007**, *129*, 12563–12570.
(21) Beaumont, E.; Lambry, J. C.; Wang, Z. Q.; Stuehr, D. J.; Martin, J. L.; Slama-Schwok, A. *Biochemistry* **2007**, *46*, 13533–13540.
(22) Wang, Z. Q.; Wei, C. C.; Sharma, M.; Pant, K.; Crane, B. R.; Stuehr, D. J. *J. Biol. Chem.* **2004**, *279*, 19018–19025.

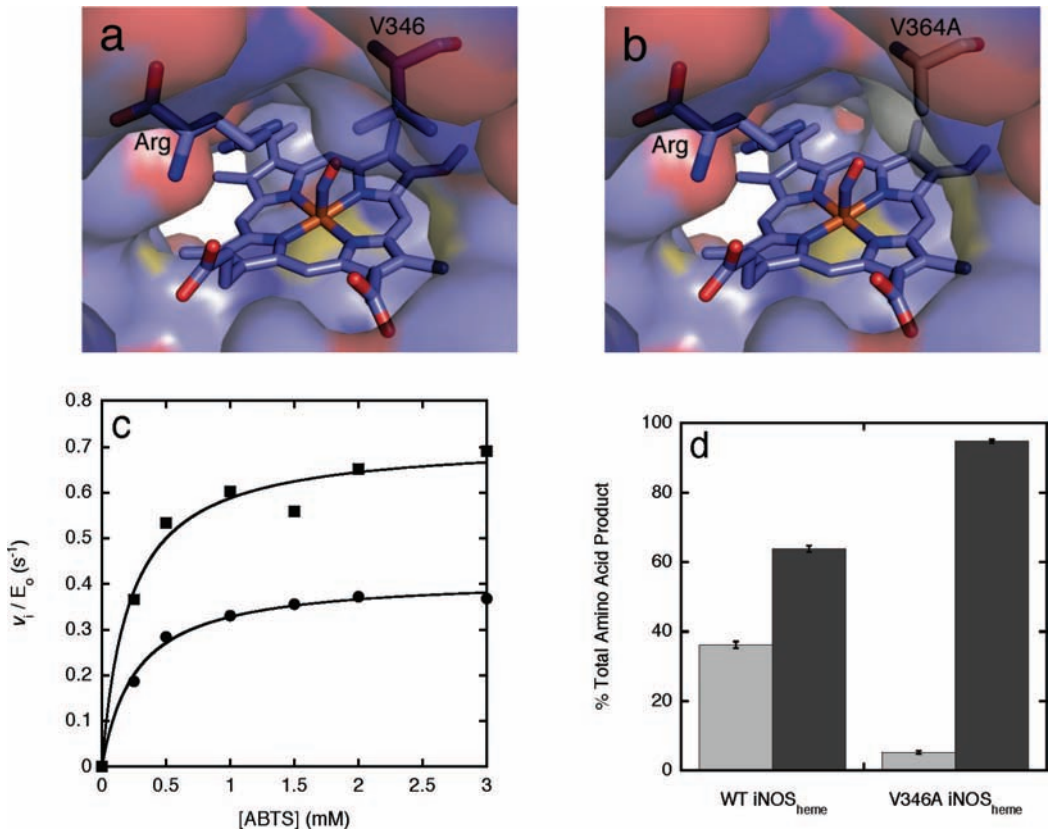

Figure 3. Peroxidase and peroxide shunt characterization of V346A iNOS$_{heme}$. (a) Solvent view of NOS active site depicting a heme bound NO, substrate arginine, and valine 346 (adapted from Li et al.). Valine 346 is a conserved residue that is positioned at the entrance of the active site of the eukaryotic NOSs. (b) Pymol model of V346A iNOS$_{heme}$ mutant depicting the opening of the entrance to the active site. (c) Steady state peroxidase activity of the V346A mutant (-■-) and wild type iNOS$_{heme}$ (-●-). Wild type data are as reported in Figure 2a. Mutant reactions contain V346A iNOS$_{heme}$ (0.37 μM), H_2O_2 (50 mM), HEPES (100 mM, pH 7.5), and variable ABTS at 10 °C. Initial rates (v_i) as determined by steady state analysis are normalized to enzyme concentration (E_o) and plotted as a function of ABTS substrate concentration. (d) CN-ornithine formation in the V346A mutant compared to wild type. Wild type data are shown in Figure 2b. V346A reactions contain protein (2 μM), H_2O_2 (100 mM), NHA (1 mM), and HEPES (100 mM, pH 7.5). Amino acids citrulline (light gray) and CN-ornithine (dark gray) are reported as the % of the total amino acid products detected.

ment in peroxide processing, this mutant exhibits enhanced peroxidase activity relative to the wild type protein (Figure 3c and Table 1). Interestingly, the amino acid products formed during peroxide shunt turnover with V346A are also significantly affected, with nearly exclusive formation of the CN-orn product (Figure 3d and Table 1).

Heme Substitution. The direct involvement of the heme in NOS catalysis suggests that the electronics of the heme will influence the reaction with H_2O_2. Heme substitution offers a direct method to alter the electronics of the heme cofactor. To examine the effect of heme on the reaction, the peroxide shunt product distribution and peroxidase activity catalyzed by Fe-MPIX and Mn-PPIX substituted iNOS$_{heme}$ were examined.

Saturation of the heme vinyl substituents to ethyl groups increases the electron density on the metal center as evidenced by a decrease in the redox potential (up to ~50 mV) in Fe-MPIX substituted proteins.[23−25] Increased electron density on the metal center should increase the rate of heterolysis to Cpd I by enhancing the "push effect,"[26] while also stabilizing the resulting Cpd I species. With peroxidases, meso-heme substitution leads to increases in peroxide cleavage.[23,27] Here, Meso-iNOS$_{heme}$ (iron mesoporphyrin IX substituted iNOS$_{heme}$) also shows enhanced peroxidase activity (Supporting Information), although saturation was not attained, and an accurate measure of the peroxidase activity was precluded.

The enhanced rate of H_2O_2 breakdown observed in other Fe-MPIX substituted proteins is predicted to increase the amount of the Fe^{IV}═O($por^{\bullet+}$) under steady-state conditions and to alter the amino acid product distribution accordingly. Indeed, Meso-iNOS$_{heme}$ produces higher levels of the product CN-orn relative to the wild-type protein (Figure 4 and Table 1), consistent with enhanced peroxidase activity. However, increased basicity on the heme iron will not only alter the peroxidase activity but may also enhance the nucleophilicity of the ferric bound peroxide, preventing a clear comparison between peroxidase activity and product distribution. Nevertheless, the dependency of the product distribution on the specific porphryin bound to the protein establishes the branch point for CN-orn and citrulline formation as a heme-dependent intermediate. The proposed mechanism of citrulline and CN-orn formation predicts that the

(23) Ryabova, E. S.; Rydberg, P.; Kolberg, M.; Harbitz, E.; Barra, A. L.; Ryde, U.; Andersson, K. K.; Nordlander, E. *J. Inorg. Biochem.* **2005**, *99*, 852–863.
(24) Wang, N.; Zhao, X.; Lu, Y. *J. Am. Chem. Soc.* **2005**, *127*, 16541–16547.
(25) Flaherty, M. M.; Rush, K. R.; Smith, A.; Crumbliss, A. L. *Biometals* **2008**, *21*, 239–248.
(26) Dawson, J. H.; Holm, R. H.; Trudell, J. R.; Barth, G.; Linder, R. E.; Bunnenberg, E.; Djerassi, C.; Tang, S. C. *J. Am. Chem. Soc.* **1976**, *98*, 3707–3709.
(27) Modi, S.; Behere, D. V. *Biometals* **1997**, *10*, 23–26.

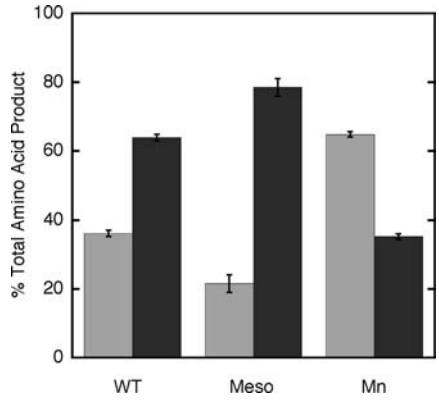

Figure 4. Peroxide shunt characterization of Fe-MPIX and Mn-PPIX substituted $iNOS_{heme}$. Meso-$iNOS_{heme}$ (Meso) favors increased CN-ornithine (dark gray) over citrulline (light gray) relative to wild type (WT), while Mn-$iNOS_{heme}$ (Mn) produces citrulline as the major amino acid product. Heme substituted reactions contain Meso-$iNOS_{heme}$ or Mn-$iNOS_{heme}$ (2 μM), H_2O_2 (100 mM), NHA (1 mM), and HEPES (100 mM, pH 7.5). Amino acids were derivatized by NDA and quantified by HPLC. Values are reported as the % of the total amino acid products detected. Wild type data are reported in Figure 2b.

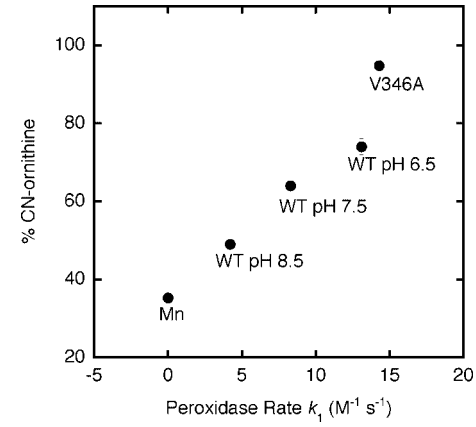

Figure 5. Peroxide breakdown rate (k_1) is correlated with CN-ornithine formation. Rates of peroxidase activity as assessed by ABTS oxidation versus the amount of CN-ornithine (% of total amino acid products) formed as reported in Table 1. V36A, V346A $iNOS_{heme}$; WT, wild type; Mn, Mn-$iNOS_{heme}$.

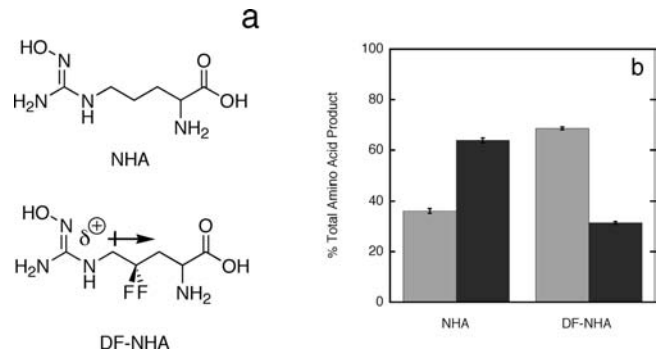

Figure 6. 4,4-Difluoro-N^G-hydroxy-L-arginine (DF-NHA) as a substrate in the peroxide shunt. (a) Structures showing the difluoro substitution on C4 of NHA. (b) Product distribution of the peroxide shunt with NHA and DF-NHA. Urea product formation is increased with DF-NHA as substrate. Data for NHA are reported in Figure 2b. Peroxide shunt reactions for the substrate analogue contain $iNOS_{heme}$ (2 μM), H_2O_2 (100 mM), DF-NHA (1 mM), and HEPES (100 mM, pH 7.5). Amino acids citrulline and 4,4-difluoro citrulline (light gray) and CN-ornithine and 4,4-difluoro-N^G-cyano-ornithine (dark gray) reported as the % of total amino acid products detected.

products are dependent on which heme bound oxidant reacts with NHA (Scheme 4). These two separate products are derived from the same ferric-peroxo intermediate, consistent with the observation of a heme dependence on product distribution.

Metal substitution was also used to investigate the role of the heme in these oxidative reactions. Mn-PPIX has a much lower redox potential than Fe-PPIX and has been used to directly observe high-valent states of P450s.[28] However, Mn substituted peroxidases have very little activity due to enhanced stability of the porphyrin-bound peroxide, leading to little formation of the Mn^V=O intermediate during steady-state turnover.[29] Consistent with this stability, no detectable peroxidase activity is observed with Mn-$iNOS_{heme}$. However, oxidation of NHA is observed during peroxide shunt reactions, with the major fraction of amino acid product being citrulline (Figure 4 and Table 1). Again, the formation of CN-orn correlates with the ability of the protein to breakdown H_2O_2. Interestingly, when the peroxide break down data is compared with the formation of CN-orn, a near linear trend becomes apparent between peroxidase activity and the production of CN-orn (Figure 5).

Substrate Electronics. Because of the proposed reaction between substrate and the ferric-peroxo intermediate, the electronics of NHA might influence the peroxide shunt product distribution. Therefore, the effect of 4,4-difluoro-N^G-hydroxy-L-arginine (DF-NHA), an NHA analogue that contains two strongly withdrawing fluorine atoms on the C4 of NHA, was examined (Figure 6a). In this case a drastic shift toward the formation of the urea product occurred with a near complete reversal of the amount of urea to cyanamide observed with NHA (Figure 6b and Table 1).

The reactivity of the substrate will affect the product distribution when the substrate directly interacts with the intermediate that is the branch point between the two pathways. It is unlikely that DF-NHA facilitates the breakdown of the heme bound peroxide. Because the ferric-peroxo species is postulated to directly attack NHA to form citrulline, improved electrophilicity of the substrate should increase flux through the nucleophilic reaction relative to the high valent pathway. As a result, the production of higher levels of citrulline over the side product CN-orn would be expected, which was what we observed.

Conclusions

In this study, the conditions favoring citrulline formation during the H_2O_2 driven oxidation of NHA by NOS were determined. Further, the peroxidase activity of $iNOS_{heme}$ was measured under various conditions as a means of directly monitoring flux through the high-valent intermediate. Hydrogen peroxide O−O bond scission catalyzed by NOS was shown to be pH, protein, and heme dependent. Further, the correlation between H_2O_2 breakdown as measured by ABTS oxidation and the fraction of the CN-orn produced in the peroxide shunt reaction (Figure 5) is consistent with the hypothesis that an Fe^{IV}=O(por$^{\bullet+}$) initiates the transformation of NHA to CN-ornithine and, consequently, that a ferric peroxo intermediate is the active oxidant in citrulline formation (Scheme 4, path a).

The activation of molecular oxygen is a universal method employed by P450 heme proteins to catalyze oxidative chemistry. However, because electron transfer to the ferric-superoxo

(28) Gelb, M. H.; Toscano, W. A.; Sligar, S. G. *Proc. Natl. Acad. Sci. U.S.A.* **1982**, *79*, 5758–5762.
(29) Low, D. W.; Abedin, S.; Yang, G.; Winkler, J. R.; Gray, H. B. *Inorg. Chem.* **1998**, *37*, 1841–1843.

intermediate is rate limiting, evaluation of the ferric-peroxo and the Fe^{IV}═O(por$^{\bullet+}$) species under catalytic turnover conditions has been difficult, necessitating the use of alternative chemical methods.

The reaction of H_2O_2 with NOS closely mimics the natural reaction pathway and is an attractive probe for examining heme-catalyzed oxidations. The use of H_2O_2 curtails the need for external electron delivery, making it more useful than the natural substrate, O_2, with enzymes in which the active site has been modified. This is critical because heme substitution, mutagenesis, and pH can all change the electron transfer steps necessary for O_2 activation. Such effects can potentially limit electron transfer and enhance uncoupling to produce $O_2^{\bullet-}$, making it much more difficult to study O−O bond activation independently.

In this report we show that H_2O_2 provides access to both the ferric-peroxo and the high-valent Fe^{IV}═O(por$^{\bullet+}$) species. Indeed, as we have shown here, the ability to access both of the potential active oxidants is complicated but illuminating. By coupling these studies with a reporter substrate (ABTS) to directly assess O−O bond scission, we have elucidated a chemical means of discriminating between the high valent and peroxo pathways that makes it possible to interrogate these complicated reactions.

Acknowledgment. We thank the members of the Marletta laboratory for critical reading and useful suggestions during the preparation of this manuscript. This work was supported by the Aldo DeBenedictis Fund, the Natural Sciences and Engineering Council of Canada, and the Alberta Heritage Foundation for Medical Research.

Supporting Information Available: Peroxidase curve fitting, peroxidase steady state kinetics derivations, peroxidase data simulations, and supporting discussion and data. This material is available free of charge via the Internet at http://pubs.acs.org.

JA807299T